PAPER

Low Complexity Overloaded MIMO Non-Linear Detector with Iterative LLR Estimation

Satoshi DENNO[†a)], ***Senior Member***, **Shuhei MAKABE**[†], ***Nonmember***, ***and*** **Yafei HOU**[†], ***Senior Member***

SUMMARY This paper proposes a non-linear overloaded MIMO detector that outperforms the conventional soft-input maximum likelihood detector (MLD) with less computational complexity. We propose iterative log-likelihood ratio (LLR) estimation and multi stage LLR estimation for the proposed detector to achieve such superior performance. While the iterative LLR estimation achieves better BER performance, the multi stage LLR estimation makes the detector less complex than the conventional soft-input maximum likelihood detector (MLD). The computer simulation reveals that the proposed detector achieves about 0.6 dB better BER performance than the soft-input MLD with about half of the soft-input MLD's complexity in a 6×3 overloaded MIMO OFDM system.

key words: *overloaded MIMO, non-linear detector, soft-input decoding, noise cancellation, ordering, complexity reduction*

1. Introduction

Communication speed has been raised to about Gbps by using many cutting-edge techniques even in wireless communication systems. Among them, multiple input multiple output (MIMO) spatial multiplexing has been playing an important role in enhancing communication speed [1]–[3]. For the enhancement, many MIMO techniques have been proposed such as serial interference cancellers based on the minimum mean square error (MMSE), precoders, iterative decoders, and so on [4]–[7]. To multiply the throughput enhancement, lots of antennas are installed on the base station in the 5G cellular system, which is called "Massive MIMO" [8]–[10]. While those techniques achieve superior performance [11]–[13], another approach has been investigated that multiplexes more signals than a degree of freedom for enhancing the transmission speed. For instance, non-orthogonal multiple access [14]–[19], faster-than-Nyquist (FTN) [20], and overloaded MIMO spatial multiplexing [21] have been investigated, and their superior performances have been revealed. If a transmitter has many antennas, overloaded MIMO makes it possible to increase the number of spatially multiplexed signal streams to that of the antennas on the transmitter in spite of the number of the receive antennas. Since many antennas are installable on base stations in the current and future cellular systems, overloaded MIMO can be regarded as one of promising techniques to increase the download throughput. Since overloaded MIMO imposes receivers to handle a detection problem in underdetermined systems, non-linear detectors have been mainly considered [21]–[29]. Linear detectors have been investigated for complexity reduction such as lattice reduction-aided MMSE receivers [30]. Iterative receivers in conjunction with linear detectors have been proposed to improve the transmission performance [31]. Although the iterative receives achieves the transmission performance comparative to the soft-input maximum likelihood detector (MLD), many iterations needed for the performance delays the signals to be output from the detectors, which increases latency in networks.

This paper proposes a non-linear overloaded MIMO detector that outperforms the soft-input MLD*. The proposed detector can be implemented with less computational complexity than the soft-input MLD. The proposed detector applies two types of techniques for achieving better transmission performance with less complexity. One is to achieve better transmission performance, which consists of an iterative log-likelihood ratio (LLR) estimation with noise cancellation and an ordering technique. The other is to reduce the complexity for making the proposed detector less complex than the soft-input MLD, which is named multi stage noise cancellation. Although the proposed detector iterates LLR estimation with noise cancellation for performance improvement, the proposed detector achieves that superior performance within two iterations, which limits the increase in latency and in complexity.

Throughout the paper, j, c^*, $\Re[c]$, and $\Im[c]$ represent the imaginary unit, complex conjugate, a real part, and an imaginary part of a complex number c. Superscript T and H indicate transpose and Hermitian transpose of a matrix or a vector, respectively. $\mathrm{tr}[\mathbf{A}]$ and $\mathrm{E}[c]$ indicate a trace of a matrix $\mathbf{A}$ and the ensemble average of c,

2. System Model

We assume that a transmitter with N_T antennas sends signals for a receiver with N_R antennas. When the transmitter and the receiver are placed on a base station and a terminal respectively, this signal transmission corresponds to that in a downlink. Since massive MIMO is currently applied in the wireless systems, the number of the antennas on the base

Manuscript received July 8, 2023.
Manuscript revised September 1, 2023.
Manuscript publicized January 30, 2024.

[†]The authors are with Faculty of Environmental, Life, Natural Science and Technology, Okayama University, Okayama-shi, 700-8530 Japan.
a) E-mail: denno@okayama-u.ac.jp

DOI: 10.23919/transcom.2023EBP3118

*A part of the ideas proposed in the paper has been presented in the conference paper [32]. However, the detail of that part is brushed up in this paper. In addition, this paper proposes the other ideas that were not included in the conference paper.

station is usually bigger than that on the terminal, which corresponds that the number of the transmit antennas is greater than that of the receive antennas, i.e., $N_{\mathrm{T}} > N_{\mathrm{R}}$, in downlinks. For high speed signal transmission, we apply orthogonal frequency division multiplexing (OFDM) to the wireless system. The information bit stream is fed to a channel encoder and its output bit stream is provided to a modulator via an interleaver. The modulator output signals are provided to the N_{F} point inverse fast Fourier transform (IFFT) for OFDM. The IFFT output signals are fed to a serial-parallel converter (SP) after the cyclic prefix addition. The N_{T} signal streams from the SP converter are provided to the N_{T} antennas, respectively. The signals transmitted from the antennas are traveling fading channels and received at the antennas on the receiver with the N_{R} antennas. All the received signals are fed to the N_{F} point FFT. Let $\mathbf{Y}(k) \in \mathbb{C}^{N_{\mathrm{R}}}$ represent a received signal vector containing the kth subcarrier signals converted from all the receive antenna output signals, the received signal vector $\mathbf{Y}(k)$ is written as,

$$\mathbf{Y}(k) = \mathbf{H}(k)\mathbf{X}(k) + \mathbf{N}(k). \tag{1}$$

In (1), $\mathbf{X}(k) \in \mathbb{C}^{N_{\mathrm{T}}}$ and $\mathbf{N}(k) \in \mathbb{C}^{N_{\mathrm{R}}}$ represent a transmission signal vector and an additive white Gaussian noise vector (AWGN) at the kth subcarrier. In addition, $\mathbf{H}(k) \in \mathbb{C}^{N_{\mathrm{R}} \times N_{\mathrm{T}}}$ denotes a channel matrix at the kth subcarrier, which is defined as follows.

$$\mathbf{H}(k) = \begin{pmatrix} h_{1,1}(k) & h_{1,1}(k) & \cdots & h_{1,N_{\mathrm{T}}}(k) \\ \vdots & h_{2,2}(k) & & \vdots \\ & \vdots & \ddots & \\ h_{N_{\mathrm{R}},1}(k) & \cdots & & h_{N_{\mathrm{R}},N_{\mathrm{T}}}(k) \end{pmatrix} \tag{2}$$

$h_{i,l}(k)$ in (2) represents a frequency response at the kth subcarrier between the ith receive antenna and the lth transmit antenna, which is defined as,

$$h_{i,l}(k) = \sum_{m=0}^{N_{\mathrm{P}}-1} \hat{h}_{i,l}(m)\, \mathrm{e}^{-\mathrm{j}2\pi \frac{mk}{N_{\mathrm{F}}}}. \tag{3}$$

In (3), N_{P} and $\hat{h}_{i,j}(m) \in \mathbb{C}$ denote the number of the paths in the channel and an mth path gain in the channel between the ith receive antenna and the lth transmit antenna. Next, the soft signals calculated from the received signal vector are provided to a channel decoder to achieve better transmission performance. When the transmission signal vector $\mathbf{X}(k)$ is defined as $\mathbf{X}(k) = \left(x_1(k) \cdots x_{N_{\mathrm{T}}}(k)\right)^{\mathrm{T}}$ where $x_m(k) \in \mathbb{C}$ represents the mth transmission signal, for instance, an LLR with respect to the real part of the signal $x_m(k)$ is defined as follows[†].

[†]Based on the Bayesian rule, the LLR can be rewritten as,

$$\log \frac{P(\Re[x_m(k)] = 1|\mathbf{Y}(k))}{P(\Re[x_m(k)] = -1|\mathbf{Y}(k))} = \log \frac{P(\mathbf{Y}(k)|\Re[x_m(k)] = 1)}{P(\mathbf{Y}(k)|\Re[x_m(k)] = -1)} \frac{P(\Re[x_m(k)] = 1)}{P(\Re[x_m(k)] = -1)}$$

This means that the approximation in (4) becomes more exact, as the term $\frac{P(\Re[x_m(k)]=1)}{P(\Re[x_m(k)]=-1)}$ comes close to 1.

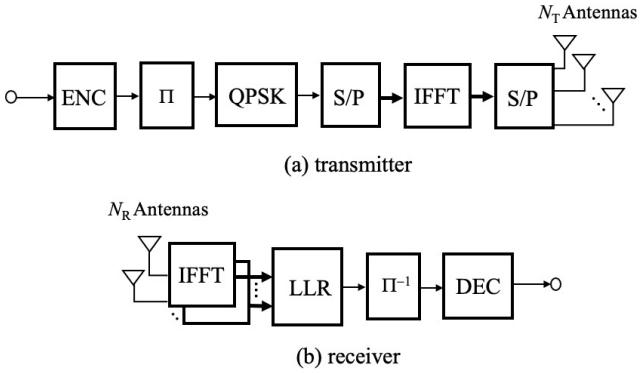

Fig. 1 System model.

$$\begin{aligned} \zeta(\Re[x_m(k)]) &= \log \frac{P(\Re[x_m(k)] = 1|\mathbf{Y}(k))}{P(\Re[x_m(k)] = -1|\mathbf{Y}(k))} \\ &\approx \log \frac{P(\mathbf{Y}(k)|\Re[x_m(k)] = 1)}{P(\mathbf{Y}(k)|\Re[x_m(k)] = -1)} \end{aligned} \tag{4}$$

$\zeta(b) \in \mathbb{R}$ and $P(c|d) \in \mathbb{R}$ in (4) denote an LLR of a signal $b \in \mathbb{R}$ and a conditional probability that an event c occurs when an event d happened. The LLR is fed to the decoder as a soft signal via a de-interleaver. The system model is illustrated in Fig. 1.

Whereas the system achieves superior transmission performance, the computational complexity grows exponentially as the number of the spatially multiplexed signal streams increases. Since the number of the spatially multiplexed signal streams is equal to that of the transmit antennas N_{T} in the system, the complexity gets higher as the number of the transmit antennas is increased. We propose a non-linear detector that achieves better transmission performance than that of the soft-input MLD, keeping complexity less than that of the soft-input MLD, in the following section.

3. Low Complexity Non-Linear Overloaded MIMO Detector

We propose two types of techniques for achieving better transmission performance with less complexity. One is to achieve better transmission performance at the cost of additional complexity. The other is to reduce the complexity for compensating the increase in complexity.

Since the same signal processing is applied to the channels on all the subcarriers, we don't need to distinguish the signal processing at one subcarrier from that at another subcarrier. The index k denoting the subcarrier number is hereafter dropped from the variables. For example, the transmission signal vector is written as $\mathbf{X}$.

3.1 Iterative LLR Estimation with Noise Cancellation

As is described in the previous section, the LLR plays a very important role in achieving the superior transmission performance. This section propose a technique to improve the quality of the LLR in the following.

First of all, the channel matrix $\mathbf{H}$ is triangulated with

the QR-decomposition for complexity reduction†.

$$\begin{pmatrix} \mathbf{H} \\ \frac{\sqrt{N_0}}{\sigma_\mathrm{d}}\mathbf{I}_{N_\mathrm{T}} \end{pmatrix} = \mathbf{QR} \tag{5}$$

In the decomposition, $\sigma_\mathrm{d} \in \mathbb{R}$, $N_0 \in \mathbb{R}$, $\mathbf{I}_{N_\mathrm{T}} \in \mathbb{C}^{N_\mathrm{T}\times N_\mathrm{T}}$, $\mathbf{Q} \in \mathbb{C}^{(N_\mathrm{R}+N_\mathrm{T})\times N_\mathrm{T}}$, and $\mathbf{R} \in \mathbb{C}^{N_\mathrm{T}\times N_\mathrm{T}}$ represent a standard deviation of the transmission signal, the double side noise power, the N_T-dimensional identity matrix, an orthogonal matrix, i.e., $\mathbf{Q}^\mathrm{H}\mathbf{Q} = \mathbf{I}_{N_\mathrm{T}}$, and an upper triangular matrix. On the other hand, the received signal vector is extended as $\dot{\mathbf{Y}} = \begin{pmatrix}\mathbf{Y}^\mathrm{T} & \mathbf{0}^\mathrm{T}\end{pmatrix}^\mathrm{T}$ where $\dot{\mathbf{Y}} \in \mathbb{C}^{(N_\mathrm{T}+N_\mathrm{R})\times 1}$ and $\mathbf{0} \in \mathbb{C}^{N_\mathrm{T}}$ represent the extended received signal vector and the N_T dimensional null vector. The extended received signal is transformed with the orthogonal matrix $\mathbf{Q}$ as,

$$\begin{aligned}\mathbf{Q}^\mathrm{H}\dot{\mathbf{Y}} &= \mathbf{Q}^\mathrm{H}\begin{pmatrix} \mathbf{H} \\ \frac{\sqrt{N_0}}{\sigma_\mathrm{d}}\mathbf{I}_{N_\mathrm{T}} \end{pmatrix}\mathbf{X} + \mathbf{Q}^\mathrm{H}\begin{pmatrix} \mathbf{N} \\ -\frac{\sqrt{N_0}}{\sigma_\mathrm{d}}\mathbf{X} \end{pmatrix} \\ &= \mathbf{RX} + \mathbf{Q}^\mathrm{H}\begin{pmatrix} \mathbf{N} \\ -\frac{\sqrt{N_0}}{\sigma_\mathrm{d}}\mathbf{X} \end{pmatrix}. \end{aligned} \tag{6}$$

Although the second term in the right hand side of (6) can be dealt as a noise vector, the vector consists of the AWGN vector and the transmission signal vector. We can expect that the signal to noise power ratio (SNR) is improved by canceling the latter part of the noise vector with the decoder output signals, which improves the quality of the LLR. Inputting the improved LLR into the decoder enhances the decoding performance. Because the higher decoding performance improves the LLR estimation performance, the LLR estimation performance is improved as the above LLR estimation procedure is iterated. Let $\bar{\mathbf{X}}^{(n)} \in \mathbb{C}^{N_\mathrm{T}}$ represent an expected transmission signal vector as a soft signal vector made from the decoder output signals at the nth iteration stage, the cancellation is defined as follows.

$$\begin{aligned}\mathbf{S}^{(n)} &= \mathbf{Q}^\mathrm{H}\dot{\mathbf{Y}} - \mathbf{Q}^\mathrm{H}\begin{pmatrix} \mathbf{0}_{N_\mathrm{T}} \\ \frac{\sqrt{N_0}}{\sigma_\mathrm{d}}\bar{\mathbf{X}}^{(n)} \end{pmatrix} \\ &= \mathbf{RX} + \mathbf{Q}^\mathrm{H}\begin{pmatrix} \mathbf{N} \\ \frac{\sqrt{N_0}}{\sigma_\mathrm{d}}\left(\bar{\mathbf{X}}^{(n)} - \mathbf{X}\right) \end{pmatrix} \end{aligned} \tag{7}$$

In (7), $\mathbf{S}^{(n)} \in \mathbb{C}^{(N_\mathrm{T}+N_\mathrm{R})\times 1}$ denotes a transformed received signal vector at the nth stage. If the received signal is transformed above, the LLR is estimated by using the MAX-log approximation as,

$$\begin{aligned}\zeta^{(n)}(\Re[x_m]) = -\frac{1}{\sigma_n^2}\Bigg(&\min_{\Re[x_m]=1}\left|\mathbf{S}^{(n)} - \mathbf{RX}\right|^2 \\ &- \min_{\Re[x_m]=-1}\left|\mathbf{S}^{(n)} - \mathbf{RX}\right|^2\Bigg). \end{aligned} \tag{8}$$

$\sigma_n^2 \in \mathbb{R}$ in (8) indicates a noise variance at the nth stage, which is defined as follows.

†The detail of the complexity reduction is explained in the next section.

$$\begin{aligned}\sigma_n^2 &= \mathrm{E}\left[\left|\mathbf{Q}^\mathrm{H}\begin{pmatrix} \mathbf{N} \\ \frac{\sqrt{N_0}}{\sigma_\mathrm{d}}(\bar{\mathbf{X}}^{(n)} - \mathbf{X}) \end{pmatrix}\right|^2\right] \\ &= \mathrm{tr}\left[\mathbf{QQ}^\mathrm{H}\mathbf{A}^{(n)}\right] \end{aligned} \tag{9}$$

$\mathbf{A}^{(n)} \in \mathbb{C}^{(N_\mathrm{R}+N_\mathrm{T})\times(N_\mathrm{R}+N_\mathrm{T})}$ in (9) represents a diagonal matrix defined as (see Appendix),

$$a^{(n)}(m,k) = \begin{cases} N_0 & m = k \le N_\mathrm{T} \\ \frac{N_0}{\sigma_\mathrm{d}^2}\left(2 - \mathrm{E}\left[\left|\bar{x}_m^{(n)}\right|^2\right]\right) & m = k > N_\mathrm{T} \\ 0 & m \ne k \end{cases} \tag{10}$$

In the above equation, $\bar{x}_m^{(n)} \in \mathbb{C}$ represents the mth element signal of the vector $\bar{\mathbf{X}}$, i.e., $\bar{\mathbf{X}}^{(n)} = \left(\bar{x}_1^{(n)} \cdots \bar{x}_{N_\mathrm{T}}^{(n)}\right)^\mathrm{T}$.

If more exact LLRs are provided to the decoder, the decoder outputs the signals with more accurate. This implies that the performance of the detection is improves as the above signal processing is iterated. We assume that the signal processing is iterated N_s times in this paper. However, the iteration causes the complexity of the signal detection to increase. The following section proposes a technique to reduce the complexity.

3.2 Multi Stage LLR Estimation

As is shown above, since the brute-force search has to be performed to find the minimum vector in the LLR estimation, the complexity of the LLR estimation is almost the same to that of the MLD. In a word, let $C_\alpha \in \mathbb{Z}$ represent the cardinality of the modulation scheme, the complexity is proportional to $C_\alpha^{N_\mathrm{T}}$. This means that the complexity can be reduced as the vector size is shrunk. We propose a complexity reduction technique of the LLR estimation by making use of the channel matrix transformed into the triangular matrix as shown in (6). For instance, let $\mathbf{S}^{(n)}(l) \in \mathbb{C}^{(N_\mathrm{T}-l+1)\times 1}$ indicate a subvector of the transformed received signal vector defined as $\mathbf{S}^{(n)}(l) = \left(s_l^{(n)} \cdots s_{N_\mathrm{T}}^{(n)}\right)^\mathrm{T}$ where $s_m^{(n)} \in \mathbb{C}$ represents the $m - l + 1$th element of the subvector $\mathbf{S}^{(n)}(l)$, the subvector $\mathbf{S}^{(n)}(l)$ contains only a part of the transmission signal vector, i.e., $\left(x_l \cdots x_{N_\mathrm{T}}\right)^\mathrm{T}$, because the channel matrix $\mathbf{R}$ is upper triangular shown in (6). If the subvector is enough for the LLR estimation with respect to the signals $x_m \quad m = l, .., N_\mathrm{T}$, the complexity will be reduced. To implement the above idea, the upper triangular matrix is decomposed as follows.

$$\mathbf{R} = \begin{pmatrix} \Pi_{(-1)\times N_\mathrm{T}}(1,1) \\ \mathbf{0} \quad \mathbf{R}(l,l) \end{pmatrix}, \tag{11}$$

where $\Pi_{(-1)\times N_\mathrm{T}}(1,1) \in \mathbb{C}^{(l-1)\times N_\mathrm{T}}$ and $\mathbf{R}(l,l) \in \mathbb{C}^{(N_\mathrm{T}-l+1)\times(N_\mathrm{T}-l+1)}$ denote a rectangular matrix and an upper sub-triangular matrix. They are defined as follows.

$$\begin{aligned}&\Pi_{(-1)\times N_\mathrm{T}}(1,1) \\ &= \begin{pmatrix} r_{1,1} & \cdots & & r_{1,N_\mathrm{T}} \\ & \ddots & \cdots & \vdots \\ 0 & & r_{l-1,l-1} & \cdots \quad r_{l-1,N_\mathrm{T}} \end{pmatrix} \end{aligned} \tag{12}$$

$$\mathbf{R}(l,l) = \begin{pmatrix} r_{l,l} & \cdots & r_{l,N_\mathrm{T}} \\ & \ddots & \vdots \\ \mathbf{0} & & r_{N_\mathrm{T},N_\mathrm{T}} \end{pmatrix} \tag{13}$$

As is shown above, a pair of the numbers in the parenthesis of the above two matrices, i.e., (n,m), indicates that the (n,m) element of the matrix $\mathbf{R}$ is the $(1,1)$ element in those matrices. If a subvector of the transmission signal vector $\mathbf{X}(l) \in \mathbb{C}^{(N_\mathrm{T}-l+1)\times 1}$ is defined as $\mathbf{X}(l) = \left(x_l\ x_{l+1} \cdots x_{N_\mathrm{T}}\right)^\mathrm{T}$, the LLR defined in (4) can be modified to the equation in (14).

$\zeta_l^{(n)}\left(\Re\left[x_{l+M^{(n)}-1}\right]\right) \in \mathbb{R}$ and $M^{(n)} \in \mathbb{Z}$ in (14) represent an LLR and a search space length. $\bar{\mathbf{X}}_{n:m} \in \mathbb{C}^{(m-n+1)\times 1}$ denotes a vector defined as $\mathbf{X}_{n:m} = (x_n \cdots x_m)^\mathrm{T}$. $\min_{a|b} f(a)$ indicates the minimum value of a function $f(a)$ with respect to a variable a under the constraint of b. In addition, $\hat{x}_i^{(n)}(\mathbf{X}_{n:m}) \in \mathbb{C}$ represents a signal dependent on the vector $\mathbf{X}_{n:m}$. In other words, if a vector $\mathbf{X}_{n:m}$ is given, a signal $\hat{x}_i^{(n)}(\mathbf{X}_{n:m})$ is uniquely got as one of the constellation points. The third term in the two minimization in (14) is composed of dependent variables $\hat{x}_i^{(n)}(\mathbf{X}_{n:m})$ which are given by the independent variables in the second term $x_i \quad i = l \cdots l+M^{(n)}-1$. Although $N_\mathrm{T}-l+1$ variables look to be included in the minimization in (14), in a word, only $M^{(n)}$ independent variables are included. The minimization with respect to only $M^{(n)}$ independent variables is carried out in (14). The search space length in the minimization is reduced from N_T to $M^{(n)}$. This makes the complexity reduced in proportion to $C_\alpha^{M^{(n)}}$, while the original LLR estimation requires the complexity proportional to $C_\alpha^{N_\mathrm{T}}$. Since $M^{(n)}$ is less than N_T, the complexity needed in (14) is much less than that of the original LLR estimation.

After the LLRs with respect to the signals $\Re\left[x_{l+M^{(n)}-1}\right]$ and $\Im\left[x_{l+M^{(n)}-1}\right]$ are obtained, next, the signal $\hat{x}_{l+M^{(n)}-1}$ is decided for every $\mathbf{X}_{l:l+M^{(n)}-2}$. In a word, $\hat{x}_{l+M^{(n)}-1}^{(n)}\left(X_{l:l+M^{(n)}-2}\right)$ is decided as follows.

$$\begin{aligned}\hat{x}_{l+M^{(n)}-1}^{(n)}\left(\mathbf{X}_{l:l+M^{(n)}-2}\right) = \underset{x_{l+M^{(n)}-1}}{\arg\min} \sum_{k=l}^{N_\mathrm{T}} \Bigg| s^{(n)}(k) \\ - \sum_{i=k}^{l+M^{(n)}-2} r_{k,i}x_i - r_{k,l+M^{(n)}-1}\, x_{l+M^{(n)}-1} \\ - \sum_{i=l+M^{(n)}}^{N_\mathrm{T}} r_{k,i}\hat{x}_i^{(n)}\left(\mathbf{X}_{l+1:l+M^{(n)}-1}\right)\Bigg|^2\end{aligned} \tag{15}$$

As is shown in (15), the signal is decided for every signal vector $\mathbf{X}_{l:l+M^{(n)}-2}$. The signal decision makes the brute force search space reduced, while keeping high transmission performance as shown below.

The multistage LLR estimation procedure is summarized as follows.

a) initialization
   $l = N_\mathrm{T} - M^{(n)} + 1$
b) LLR estimation
   Signal processing in (14) for the LLR $\zeta_l^{(n)}(\Re[x_{l+M^{(n)}-1}])$
c) Tentative signal decision
   signal decision for the possible vectors $\mathbf{X}_{l+1:k+M^{(n)}-2}$ in (15)
d) Loop control
   if $l > 1$ then
   $l = l - 1$ and go to step b)
   else
   l is fixed to 1
   LLR $\zeta_l^{(n)}(\Re[x_m])$ and $\zeta_l^{(n)}(\Im[x_m])$ estimation by using (14) where $x_{l+M^{(n)}-1}$ is replaced with x_m for $m = 1 \sim M^{(n)}$
   end

3.2.1 Ordering Based on Channel Norm

As is described in the previous section, the signal decision in (15) makes the LLR estimation less complex. However, the wrong signal decision deteriorates the LLR estimation performance. In a word, as the decision performance is improved, the LLR estimation will get more accurate. The section proposes a technique to improve the decision performance.

First of all, the matrix $\mathbf{R}(l,l)$ is redefined as $\mathbf{R}(l,l) = \left(\mathbf{R}_l(l) \cdots \mathbf{R}_{N_\mathrm{T}}(l)\right)$, where $\mathbf{R}_m(l) \in \mathbb{C}^{(N_\mathrm{T}-l+1)\times 1}$ represents $m-l+1$th column vector of the matrix $\mathbf{R}(l,l)$. We search the column vector that satisfies the following equation.

$$k_l = \underset{l \le k \le l+M^{(n)}-1}{\arg\max} \left[|\mathbf{R}_k(l)|\right] \tag{16}$$

$k_l \in \mathbb{Z}$ in (16) represents an index of the column vector. The k_lth column vector is swapped with the $l+M^{(n)}-1$th column vector in the matrix $\mathbf{R}(l)$ as,

$$\begin{aligned}\ddot{\mathbf{R}}(l,l) &= \left(\mathbf{R}_l(l) \cdots \mathbf{R}_{k_l-1}(l)\ \mathbf{R}_{l+M^{(n)}-1}(l)\ \mathbf{R}_{k_l+1}(l)\right. \\ &\quad \left. \cdots \mathbf{R}_{l+M^{(n)}-2}(l)\ \mathbf{R}_{k_l}(l)\ \mathbf{R}_{l+M^{(n)}}(l) \cdots \mathbf{R}_{N_\mathrm{T}}(l)\right) \\ &= \left(\ddot{\mathbf{R}}_l(l) \cdots \ddot{\mathbf{R}}_{N_\mathrm{T}}(l)\right).\end{aligned} \tag{17}$$

$\ddot{\mathbf{R}}(l,l) \in \mathbb{C}^{(N_\mathrm{T}-l+1)\times(N_\mathrm{T}-l+1)}$ in (17) denotes a swapped matrix[†]. Let $\hat{\mathbf{X}}(l) \in \mathbb{C}^{(N_\mathrm{T}-l+1)\times 1}$ denote a subvector defined as $\hat{\mathbf{X}}(l) = \left(x_l \cdots x_{l+M^{(n)}-1}\ \hat{x}_{l+M^{(n)}}\left(\mathbf{X}_{l+1:l+M^{(n)}-1}\right) \cdots \right.$ $\left.\hat{x}_{N_\mathrm{T}}\left(\mathbf{X}_{l+1:l+M^{(n)}-1}\right)\right)^\mathrm{T}$, the subvector is also swapped to keep the channel model in spite of the swapping of the matrix $\mathbf{R}(l,l)$, which is defined as follows.

$$\begin{aligned}\ddot{\hat{\mathbf{X}}}^{(n)}(l) &= \left(x_l \cdots x_{k_l-1}\ x_{l+M^{(n)}-1}\ x_{k_l+1} \cdots x_{l+M^{(n)}-2}\ x_{k_l}\right. \\ &\quad \left.\hat{x}_{l+M^{(n)}}\left(\mathbf{X}_{l+1:l+M^{(n)}-1}\right) \cdots \hat{x}_{N_\mathrm{T}}\left(\mathbf{X}_{l+1:l+M^{(n)}-1}\right)\right) \\ &= \left(\ddot{x}_l \cdots \ddot{x}_{l+M^{(n)}-1}\ \ddot{\hat{x}}_{l+M^{(n)}}\left(\ddot{\mathbf{X}}_{l+1:l+M^{(n)}-1}\right)\right. \\ &\quad \left. \cdots \ddot{\hat{x}}_{N_\mathrm{T}}\left(\ddot{\mathbf{X}}_{l+1:l+M^{(n)}-1}\right)\right)\end{aligned} \tag{18}$$

In (18), $\ddot{\hat{\mathbf{X}}}^{(n)}(l) \in \mathbb{C}^{(N_\mathrm{T}-l+1)\times 1}$ and $\ddot{\mathbf{X}}_{n:m} \in \mathbb{C}^{(n-m+1)\times 1}$ represent swapped vectors transformed from $\hat{\mathbf{X}}^{(n)}(l)$ and $\mathbf{X}_{n:m}$, respectively. With those vectors, the LLR is calculated and

[†]The matrix $\ddot{\mathbf{R}}(l,l)$ is not upper triangular, unless $k_l = l + M^{(n)} - 1$ at all the stages.

$$\zeta^{(n)}\left(\Re\left[x_{l+M^{(n)}-1}\right]\right)\approx \zeta_l^{(n)}\left(\Re\left[x_{l+M^{(n)}-1}\right]\right) = -\frac{1}{\sigma_n^2}\left(\min_{\Re[x_{l+M^{(n)}-1}]=1}\left|\mathbf{S}^{(n)}(l)-\mathbf{R}(l,l)\mathbf{X}(l)\right|^2 - \min_{\Re[x_{l+M^{(n)}-1}]=-1}\left|\mathbf{S}^{(n)}(l)-\mathbf{R}(l,l)\mathbf{X}(l)\right|^2\right)$$

$$\approx -\frac{1}{\sigma_n^2}\left(\min_{\substack{\mathbf{X}_{l+1:l+M^{(n)}-1}|\\ \Re\left[x_{l+M^{(n)}-1}\right]=1}}\sum_{k=l}^{N_\mathrm{T}}\left|s^{(n)}(k)-\sum_{i=k}^{l+M^{(n)}-1}r_{k,i}x_i-\sum_{i=l+M^{(n)}}^{N_\mathrm{T}}r_{k,i}\hat{x}_i^{(n)}\left(\mathbf{X}_{l+1:l+M^{(n)}-1}\right)\right|^2\right.$$

$$\left.-\min_{\substack{\mathbf{X}_{l+1:l+M^{(n)}-1}|\\ \Re\left[x_{l+M^{(n)}-1}\right]=-1}}\sum_{k=l}^{N_\mathrm{T}}\left|s^{(n)}(k)-\sum_{i=k}^{l+M^{(n)}-1}r_{k,i}x_i-\sum_{i=l+M^{(n)}}^{N_\mathrm{T}}r_{k,i}\hat{x}_i^{(n)}\left(\mathbf{X}_{l+1:l+M^{(n)}-1}\right)\right|^2\right) \tag{14}$$

the signal is decided at the nth stage based on (14) and (15) as follows.

$$\zeta_l^{(n)}(\Re[\ddot{x}_{l+M^{(n)}-1}])$$
$$= -\frac{1}{\sigma_n^2}\left(\min_{\Re[\ddot{x}_{l+M^{(n)}-1}]=1}\left|\mathbf{S}^{(n)}(l)-\ddot{\mathbf{R}}(l)\ddot{\hat{\mathbf{X}}}^{(n)}(l)\right|^2\right.$$
$$\left.-\min_{\Re[\ddot{x}_{l+M^{(n)}-1}]=-1}\left|\mathbf{S}^{(n)}(l)-\ddot{\mathbf{R}}(l)\ddot{\hat{\mathbf{X}}}^{(n)}(l)\right|^2\right) \tag{19}$$

$$\ddot{\hat{x}}^{(n)}_{k_{l+M^{(n)}-1}}\left(\ddot{\mathbf{X}}_{l:l+M^{(n)}-2}\right)$$
$$= \arg\min_{\ddot{x}_{k_{l+M^{(n)}-1}}}\sum_{k=l}^{N_\mathrm{T}}\left|s^{(n)}(k)-\sum_{i=k}^{l+M^{(n)}-2}\ddot{r}_{k,i}\ddot{x}_i\right.$$
$$\left.-\ddot{r}_{k,l+M^{(n)}-1}\,\ddot{x}_{k_{l+M^{(n)}-1}}-\sum_{i=l+M^{(n)}}^{N_\mathrm{T}}\ddot{r}_{k,i}\ddot{\hat{x}}_i^{(n)}\left(\ddot{\mathbf{X}}_{l+1:l+M^{(n)}-1}\right)\right|^2 \tag{20}$$

In (20), $\ddot{r}_{k,i}\in\mathbb{C}$ represents a $(k-l+1, i-l+1)$ element of the matrix $\ddot{\mathbf{R}}(l,l)$. When this technique is used, the LLR estimation procedure described at the end of the previous section has to be modified as follows.

e) (19) replaces (14)

f) (20) and $\ddot{\mathbf{X}}_{l+1:l+M^{(n)}-1}$ replace (15) and $\mathbf{X}_{l+1:l+M^{(n)}-1}$, respectively.

g) The following signal processing replaces "l=l-1" in the if-block at the procedure d).

$$\mathbf{R}(l-1,l-1)=\begin{pmatrix} r_{l-1,l-1} & \cdots & r_{l-1,N_\mathrm{T}}\\ 0 & \ddot{\mathbf{R}}(l,l)\end{pmatrix}$$
$$\mathbf{X}^{(n)}(l-1)=\left(x_{l-1}\quad \ddot{\hat{\mathbf{X}}}^{(n)}(l)^\mathrm{T}\right)^\mathrm{T}$$
$$l=l-1\quad\text{except for}\quad \mathbf{R}(1-1,1-1),\mathbf{X}^{(\mathrm{n})}(1-1)$$

However, the matrix $\mathbf{R}(l,l)$ at the initial stage is defined as that in (11) where $l=N_\mathrm{T}-M^{(n)}+1$. Also, the definition of the vector $\mathbf{X}^{(n)}(l)$ at the initial stage is the same to that in the previous section, i.e., $\mathbf{X}^{(n)}(l)=\mathbf{X}(l)=\left(x_l\ x_{l+1}\cdots x_{N_\mathrm{T}}\right)^\mathrm{T}$.

3.2.2 Irregular Multi Stage Configuration in Iterative LLR Estimation

As is shown in the previous section, the complexity is reduced as the search space length $M^{(n)}$ is decreased. However, increasing the search space improves the transmission performance. This means that there is a trade-off between the complexity and the transmission performance with respect to the search space length. In addition, we can change the search space length for every iteration. The combination of the search space length is described as $\left(M^{(0)}, M^{(1)}, \cdots M^{(N_\mathrm{s})}\right)$ in this paper when the LLR estimation is iterated N_s times. Then, we find out the best combination that makes the proposed non-linear detector outperforms the conventional soft-input MLD with less computational complexly. Since the theoretical performance is difficult to derive, the best combination is searched through computer simulation in the following section.

4. Computer Simulation

The performance of the proposed non-linear detector is evaluated by computer simulation in overloaded MIMO-OFDM systems. While 6 antennas are installed on the transmitter, 3 antennas are put on the receiver, i.e., the overloading ratio is 2. The modulation scheme is quaternary phase shift keying (QPSK), and a half rate convolutional code with a constraint length of 3 is used [34]. The number of the subcarriers N_F is set to 64. Multipath Rayleigh fading is applied to the channels between the transmitter and the receiver where the Jakes' model is used for each path model. The sorted QR-decomposition is applied [35]. Table 1 summarizes the simulation parameters. The soft-input MLD is referred as a conventional detector in the following performance evaluation.

Table 1 Simulation parameters.

Modulation	QPSK/OFDM
No. of subcarriers, N_F	64
Channel model	4-path Rayleigh fading
(N_T, N_R)	(6, 3)
Channel estimation	Perfect
QR-decomposition	Sorted QR-decomposition [35]
Error correction coding	Convolutional code $\left(R = \frac{1}{2}, K = 3\right)$
Decoding algorithm	Soft-input Soft-output Viterbi
Maximum No. of iterations	2

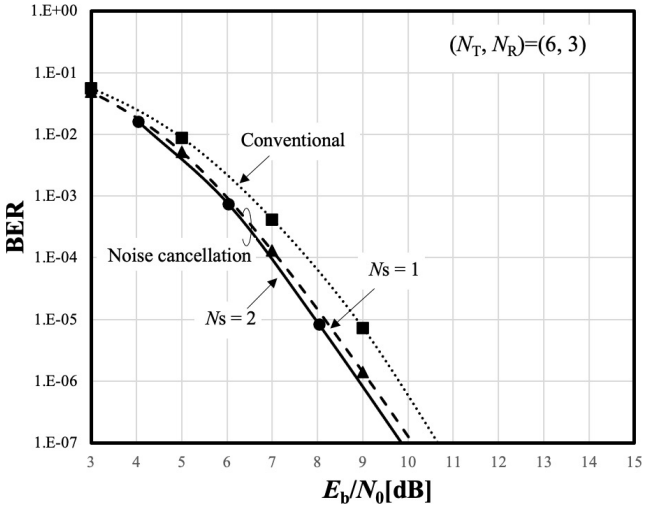

Fig. 2 BER performance of noise cancellation.

4.1 BER Performance

Figure 2 shows the BER performance of the proposed non-linear detector with the search space length $M^{(n)} = N_T = 6$ $n = 1, 2$, which corresponds to the proposed detector with the single stage LLR estimation. In other words, if the multistage LLR estimation is not used in the proposed non-linear detector, the figure shows the performance of only the LLR estimation with the noise cancellation. The performance is improved as the number of the iterations increases. As is seen, the performance gain is saturated at the second iteration, i.e., $N_s = 2$. This is the reason why the maximum number of the iterations is set to 2 in Table 1. The two-iteration attains a gain of about 1 dB at the BER of 10^{-5}.

Figure 3 shows the BER performance of the proposed non-linear detector with the number of the iteration N_s of 0. Because the LLR estimation with the noise cancellation is not employed in the detector with N_s of 0, the performance of the multistage LLR estimation in conjunction with the ordering is just confirmed. In the figure, the performance of the proposed detector without the ordering is added for a reference. As the search space length $M^{(0)}$ is decreased, the BER performance gets worse. Besides, the proposed ordering improves the performance despite of the search space length $M^{(0)}$.

Figure 4 and Fig. 5 show the BER performance of the

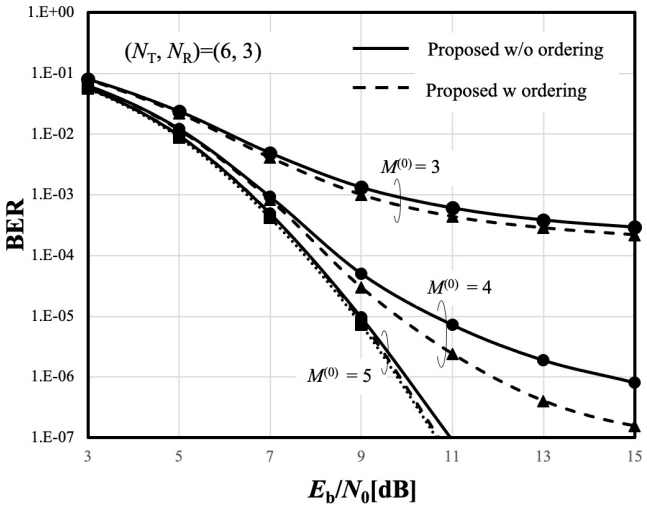

Fig. 3 BER performance ($N_s = 0$).

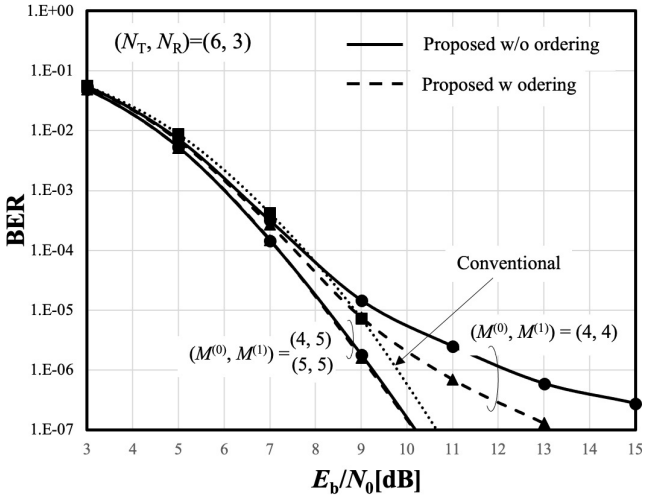

Fig. 4 BER performance ($N_s = 1$).

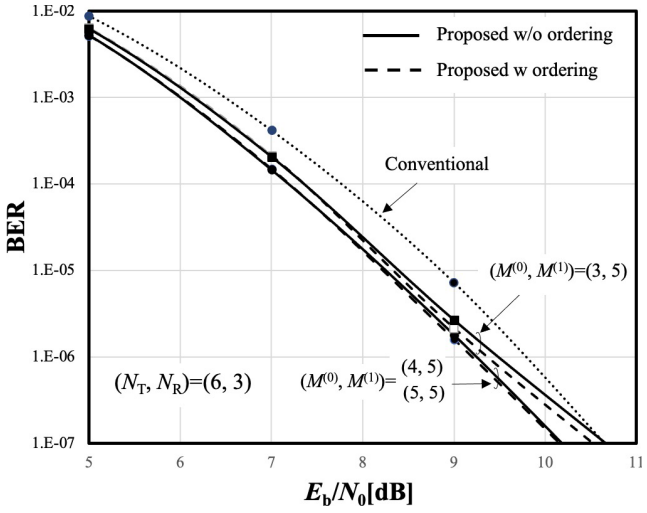

Fig. 5 BER performance ($N_s = 1$).

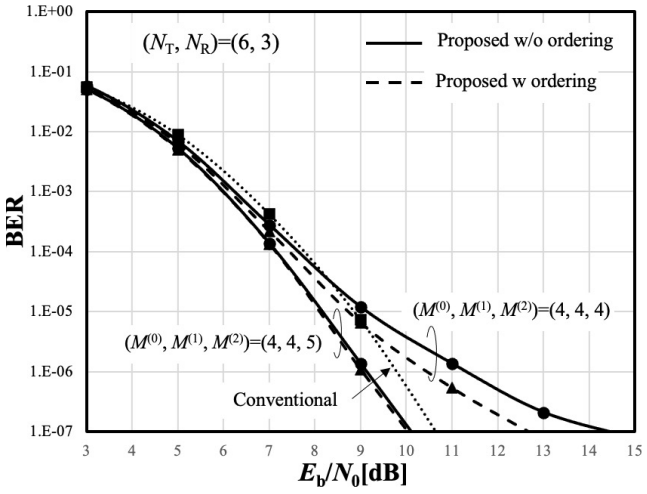

Fig. 6 BER performance (N_s = 2).

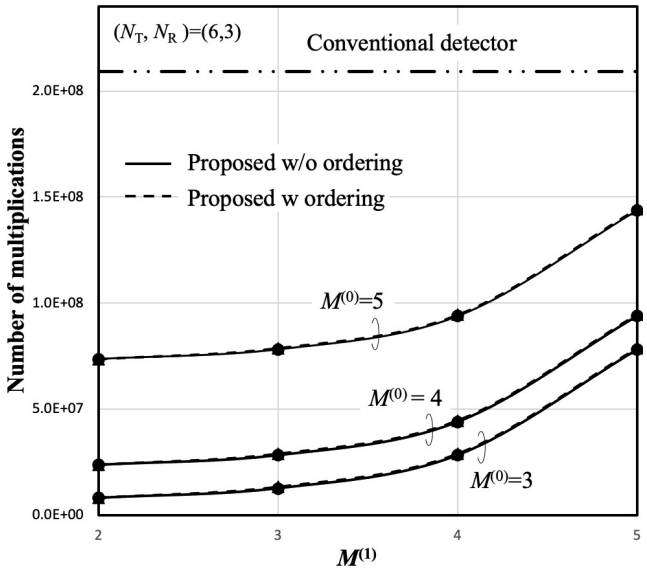

Fig. 7 Complexity (N_s = 1).

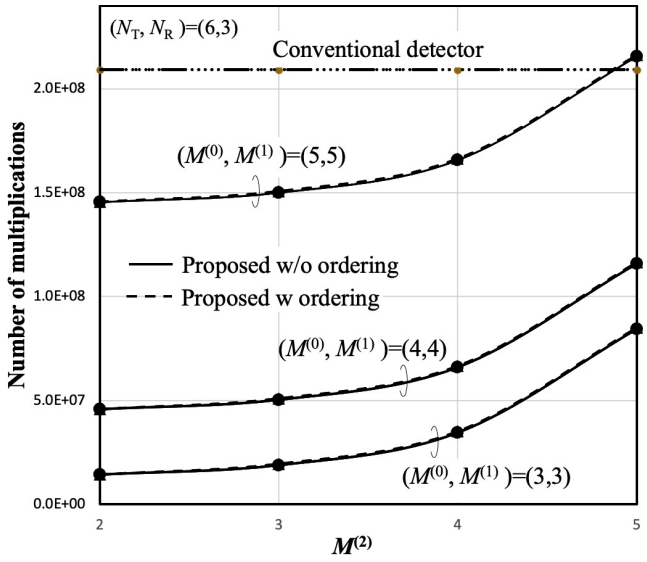

Fig. 8 Complexity (N_s = 2).

proposed detector where the LLR estimation with noise cancellation is iterated once, i.e., N_s = 1. As the search space length at the 1st iteration $M^{(1)}$ increases, the BER performance is improved. When the search space length $M^{(1)}$ is set to 5, the proposed detector achieves almost the same BER performance despite of the search space length at the 0th iteration $M^{(0)}$. Actually, as is shown in Fig. 5, even when the search space length $M^{(1)}$ is 5, the BER performance degrades at the lower BER region if the search space length $M^{(0)}$ is reduced to 3. In other words, the proposed detector with the search space length $M^{(1)}$ of 5 achieves about 0.6 dB better BER performance than the conventional soft-input MLD, as far as the search space length $M^{(0)}$ is more than 3.

Figure 6 shows the BER performance of the proposed detector with the number of the iteration N_s of 2. If the performance in Fig. 6 is compared with that in Fig. 2, we can realize that the use of the search space length $M^{(2)}$ of 5 makes the proposed detector achieve the near performance to that with $M^{(2)}$ of 6 as far as $M^{(n)}$ $n = 0, 1$ are more than 3. The proposed detector with that combination of the search space length achieve 0.7 dB better BER performance than the conventional detector.

4.2 Complexity

Figure 7 shows the complexity of the proposed non-linear detector when the number of the iterations is set to 1, i.e., N_s = 1. The complexity of the conventional detector is drawn as a reference. The ordinate is the number of the multiplications needed for detecting all the symbols in a packet, and the abscissa is the search space length $M^{(1)}$. While the complexity of the conventional detector is independent of the search space, the complexity of the proposed detector increases as the search space length $M^{(1)}$ is raised. Similarly, the complexity also depends on the search space length $M^{(0)}$. This concludes that the complexity of the proposed detector with any combinations is less than that of the conventional detector as far as the combinations shown in the figure are applied.

Figure 8 shows the complexity of the proposed non-linear detector when the number of the iteration is 2, i.e., N_s = 2. While the ordinate is the same to that in Fig. 7, the abscissa is the search space length $M^{(2)}$. $M^{(1)}$ is set to the same to $M^{(0)}$ in the figure. Although the other combinations can be thought of, the simplest combinations are investigated. Similar as the complexity in Fig. 7, the complexity is increased if not only the search space length $M^{(2)}$ but also $\left(M^{(0)}, M^{(1)}\right)$ increase. As is seen in the figure, while the complexity of the detector with $\left(M^{(0)}, M^{(1)}, M^{(2)}\right) = (5,5,5)$ exceeds that of the conventional detector, the complexity of the other combinations is less than that of the conventional detector. This means that the proposed detector can

be implemented with less complexity than the conventional detector unless $\left(M^{(0)}, M^{(1)}, M^{(2)}\right) = (5,5,5)$.

Consequently, when the LLR estimation with noise cancellation is iterated less than three times, the proposed detector achieves about 0.7 dB better BER performance than the soft-input MLD at most, even though the complexity of the detector is less than the soft-input MLD, unless the search spaces length $\left(M^{(0)}, M^{(1)}, M^{(2)}\right) = (5,5,5)$ is used. Especially, even though the performance gain is a little bit reduced to about 0.6 dB, the complexity of the proposed detector can be reduced to about half of that of the complexity by iterating the LLR estimation once in the proposed detector with the search space length $\left(M^{(0)}, M^{(1)}\right) = (4,5)$.

Although the complexity of the proposed non-linear detector is compared with that of the proposed nonlinear detector without ordering in Fig. 7 and Fig. 8, the two performances are almost overlapped, which means that the complexity needed for the ordering is negligible small compared with that for the multi stage LLR estimation. In a word, the ordering can be implemented with negligible small additional complexity.

While the performance gain is not guaranteed in practical systems, the complexity reduction shown above is achieved in any systems. When the detector with less complex than the MLD is needed, it is better to start with small search space length. If the gain is not sufficient in a practical system, the search space length should be increased until enough performance gain is obtained.

5. Conclusion

This paper has proposed a non-linear MIMO detector for overloaded MIMO channels. The proposed non-linear MIMO detector achieves better BER performance than the conventional soft-input MLD with less computational complexity. The proposed detector performs iterative multistage LLR estimation with noise cancellation for achieving such superior performance. Furthermore, we propose ordering based on the channel norm to enhance the transmission performance of the proposed detector. While the iterative LLR estimation with noise cancellation achieves better estimation performance as the number of the iterations increases, the multistage LLR estimation reduces the computational complexity, which compensates the complexity increased by the iterative LLR estimation. An irregular multi stage configuration has been considered to find the best configuration that makes the proposed detector achieve better transmission performance than the conventional soft-input MLD with less computational complexity.

The performance of the proposed non-linear MIMO detector is evaluated by computer simulation in a 6×3 overloaded MIMO-OFDM system. The proposed non-linear detector achieves about 0.6 dB better BER performance than the conventional soft-input MLD, even though the computational complexity is about half as much as that of the soft-input MLD, when the LLR estimation is iterated once with the search space length $\left(M^{(0)}, M^{(1)}\right)$ of $(4,5)$.

Acknowledgments

The work has been supported by JSPS KAKENHI JP21K04061, the support center for advanced telecommunications technology research (SCAT), and Softbank Co. ltd.

References

[1] G.J. Foschini and M.J. Gans, "On limits of wireless communications in a fading environment when using multiple antennas," Wireless Pers. Commun., vol.6, no.3, pp.311–335, 1998.
[2] I.E. Telater, "Capacity of multi-antenna Gaussian channels," European Transactions on Telecommunications, vol.10, no.6, pp.585–595, 1999.
[3] S. Yang and L. Hanzo, "Fifty years of MIMO detection: The road to large-scale MIMOs," IEEE Commun. Surveys Tuts., vol.17, no.4, pp.1941–1988, Fourthquarter 2015.
[4] G.J. Foschini, "Layered space-time architecture for wireless communication in a fading environment when using multiple antennas," Bell Lab. Tech. J., vol.1, no.2, pp.41–59, 1996.
[5] P.W. Wolniansky, G.J. Foschini, G.D. Golden, and R.A. Valenzuela, "V-BLAST: An architecture for realizing very high data rates over the rich-scattering wireless channel," Proc. IEEE ISSSE-98, Pisa, Italy, Sept. 1998.
[6] Q.H. Spencer, A.L. Swindlehurst, and M. Haardt, "Zero-forcing methods for downlink spatial multiplexing in multiuser MIMO channels," IEEE Trans. Signal Process., vol.52, no.2, pp.461–471, 2004.
[7] T. Abe, S. Tomisato, and T. Matsumoto, "A MIMO turbo equalizer for frequency-selective channels with unknown interference," IEEE Trans. Veh. Technol., vol.53, no.3, pp.476–482, 2003.
[8] E.G. Larsson, O. Edfors, F. Tufvesson, and T.L. Marzetta, "Massive MIMO for next generation wireless systems," IEEE Commun. Mag., vol.52, no.2, pp.186–195, Feb. 2014.
[9] M. Sakai, K. Kamohara, H. Iura, H. Nishimoto, K. Ishioka, Y. Murata, M. Yamamoto, A. Okazaki, N. Nonaka, S. Suyama, J. Mashino, A. Okamura, and Y. Okumura, "Experimental field trials on MU-MIMO transmissions for high SHF wide-band massive MIMO in 5G," IEEE Trans. Wireless Commun., vol.19, no.4, pp.2196–2207, April 2020.
[10] L. Lu, G.Y. Li, A.L. Swindlehurst, A. Ashikhmin, and R. Zhang, "An overview of massive MIMO: Benefits and challenges," IEEE J. Sel. Topics Signal Process., vol.8, no.5, pp.742–758, Oct. 2014.
[11] P. Som, T. Datta, A. Chockalingam, and B.S. Rajan, "Improved large-MIMO detection based on damped belief propagation," IEEE Information Theory Workshop on Information Theory (ITW), 2010.
[12] W. Fukuda, T. Abiko, T. Nishimura, T. Ohgane, Y. Ogawa, Y. Ohwatari, and Y. Kishiyama, "Low-complexity detection based on belief propagation in a massive MIMO system," IEEE 77th Vehicular Technology Conference (VTC Spring), 2013.
[13] T. Takahashi, S. Ibi, and S. Sampei, "On normalization of matched filter belief in GaBP for large MIMO detection," IEEE 84th Vehicular Technology Conference (VTC-Fall), 2016.
[14] R. Hoshyar, F.P. Wathan, and R. Tafazolli, "Novel low-density signature for synchronous CDMA systems over AWGN channel," IEEE Trans. Signal Process., vol.56, no.4, pp.1616–1626, April 2008.
[15] R. Stoica, G. Abreu, Z. Liu, T. Hara, and K. Ishibashi, "Massively concurrent non-orthogonal multiple access for 5G networks and beyond" IEEE Access, vol.7, pp.82080–82100, June 2019.
[16] S.M.A. Kazmi, N.H. Tran, T.M. Ho, D. Niyato, and C.S. Hong, "Coordinated device-to-device communication with non-orthogonal multiple access in future wireless cellular networks," IEEE Access, vol.6, pp.39860–39875, June 2018.

[17] K. Higuchi and A. Benjebbour, "Non-orthogonal multiple access (NOMA) with successive interference cancellation for future radio access," IEICE Trans. Commun., vol.E98-B, no.3, pp.403–414, March 2015.
[18] Y. Liu, Z. Qin, M. Elkashlan, Z. Ding, A. Nallanathan, and L. Hanzo, "Nonorthogonal multiple access for 5G and beyond," Proc. IEEE, vol.105, no.12, pp.2347–2381, Dec. 2017.
[19] H. Yang, X. Fang, Y. Liu, X. Li, Y. Luo, and D. Chen, "Impact of overloading on link-level performance for sparse code multiple access," 25th Wireless and Optical Communication Conference (WOCC), 2016.
[20] M. Anan, M. Sawahashi, and Y. Kishiyama, "BLER performance of windowed-OFDM using faster-than-Nyquist signaling with 16QAM," 21st International Symposium on Wireless Personal Multimedia Communications (WPMC), 2018.
[21] K.K. Wong, A. Paulraj, and R.D. Murch, "Efficient high-performance decoding for overloaded MIMO antenna systems," IEEE Trans. Wireless Commun., vol.6, no.5, pp.1833–1843, May 2007.
[22] N. Surajudeen-Bakinde, X. Zhu, J. Gao, and A.K. Nandi, "Improved signal detection approach using genetic algorithm for overloaded MIMO systems," 4th International Conference on Wireless Communications, Networking and Mobile Computing, 2008.
[23] X. Lian and D. Li, "On the application of sphere decoding algorithm in overload MIMO systems," IEEE International Conference on Information Theory and Information Security, Dec. 2010.
[24] I. Shubhi and Y. Sanada, "Joint turbo decoding for overloaded MIMO-OFDM systems," IEEE Trans. Veh. Technol., vol.66, no.1, pp.433–442, Jan. 2017.
[25] R. Shioji, T. Imammura, and Y. Sanada, "Overloaded MIMO detection based on two-stage belief propagation with MMSE precancellation," Proc. IEEE Vehicular Technol. Conf. (VTC2021-Fall), Sept. 2021.
[26] S. Yoshikawa, S. Denno, and M. Morikura, "Complexity reduced lattice-reduction-aided MIMO receiver with virtual channel detection," IEICE Trans. Commun., vol.E96-B, no.1, pp.263–270, Jan. 2013.
[27] R. Hayakawa, K. Hayashi, and M. Kaneko, "Lattice reduction-aided detection for overloaded MIMO using slab decoding," IEICE Trans. Commun., vol.E99-B, no.8, pp.1697–1705, Aug. 2016.
[28] R. Hayakawa and K. Hayashi, "Convex optimization-based signal detection for massive overloaded MIMO systems," IEEE Trans. Wireless Commun., vol.16, no.11, pp.7080–7091, Nov. 2017.
[29] T. Takahashi, S. Ibi, A. Tölli, and S. Sampei, "Subspace marginalized belief propagation for mmWave overloaded MIMO signal detection," Proc. IEEE Intern. Conf. Commun. (ICC2020), June 2020.
[30] S. Denno, Y. Kawaguchi, H. Murata, and D. Umehara, "An iterative noise cancelling receiver with soft-output LR-aided detection for collaborative reception," Proc. 19th International Symposium on Wireless Personal Multimedia Communications (WPMC 2016), Shenzhen China, Nov. 2016.
[31] S. Denno, T. Inoue, T. Fujiwara, and Y. Hou, "Low complexity soft input decoding in an iterative linear receiver for overloaded MIMO," IEICE Trans. Commun., vol.E103-B, no.5, pp.600–608, May 2020.
[32] S. Makabe, S. Denno, and Y. Hou, "A low complexity non-linear iterative receiver for overloaded MIMO-OFDM systems," Proc. 2022 27th Asia Pacific Conference on Communications (APCC), pp.488–493, Jeju Island, Korea, 2022.
[33] T. Abe and T. Matsumoto, "Space-time turbo equalization in frequency-selective MIMO channels," IEEE Trans. Veh. Technol., vol.52, no.3, pp.469–475, 2003.
[34] J.G. Proakis and M. Salehi, Digital Communications, 5th ed., McGraw-Hill, 2008.
[35] D. Wübben, R. Böhnke, V. Kühn, and K.-D. Kammeyer, "MMSE extension of V-BLAST based on sorted QR decomposition," Proc. IEEE Veh. Technolol. Conf. (VTC2003-Fall), Orland Fl, USA, Oct. 2003.

Appendix: Devivation of (10)

When we see (9), the matrix $\mathbf{A}^{(n)}$ can be written from as follows.

$$\mathbf{A}^{(n)} = \mathrm{E}\left[\begin{pmatrix} \mathbf{N} \\ \frac{\sqrt{N_0}}{\sigma_\mathrm{d}}(\bar{\mathbf{X}}^{(n)} - \mathbf{X}) \end{pmatrix}\begin{pmatrix} \mathbf{N} \\ \frac{\sqrt{N_0}}{\sigma_\mathrm{d}}(\bar{\mathbf{X}}^{(n)} - \mathbf{X}) \end{pmatrix}^{\mathrm{H}}\right]$$
$$= \begin{pmatrix} \mathrm{E}\left[\mathbf{N}\mathbf{N}^{\mathrm{H}}\right] & \mathbf{0}_{N_\mathrm{R}\times N_\mathrm{T}} \\ \mathbf{0}_{N_\mathrm{T}\times N_\mathrm{R}} & \frac{N_0}{\sigma_\mathrm{d}^2}\mathrm{E}\left[(\bar{\mathbf{X}}^{(n)} - \mathbf{X})(\bar{\mathbf{X}}^{(n)} - \mathbf{X})^{\mathrm{H}}\right] \end{pmatrix} \quad (\mathrm{A}\cdot 1)$$

In the above derivation, we use the characteristics that the AWGN and the transmission signals are uncorrelated, Because the transmission signals are generated independently, the correlation between one symbol and the other symbol becomes zero. This means that the matrix $\mathrm{E}\left[(\bar{\mathbf{X}}^{(n)} - \mathbf{X})(\bar{\mathbf{X}}^{(n)} - \mathbf{X})^{\mathrm{H}}\right]$ is reduced to a diagonal matrix. The diagonal element can be rewritten as $\mathrm{E}\left[\left|\bar{x}_m^{(n)} - x_m\right|^2\right] = \mathrm{E}\left[\left|\Re\left[\bar{x}_m^{(n)}\right] - \Re\left[x_m\right]\right|^2 + \left|\Im\left[\bar{x}_m^{(n)}\right] - \Im\left[x_m\right]\right|^2\right]$. Because the QPSK is applied, $\Re\left[\bar{x}_m^{(n)}\right]$ and $\Im\left[\bar{x}_m^{(n)}\right]$ are soft output bits coming out from the decoder. Let b and $\bar{b}$ denote a transmission antipodal bit and a decoder soft output bit respectively, the following relation is known; $\mathrm{E}\left[\left|\bar{b} - b\right|^2\right] = 1 - \mathrm{E}\left[\bar{b}^2\right]$ [33]. Hence, (10) can be obtained.

Satoshi Denno received the M.E. and Ph.D. degrees from Kyoto University, Kyoto, Japan in 1988 and 2000, respectively. He joined NTT radio communications systems labs, Yokosuka, Japan, in 1988. He was seconded to ATR adaptive communications research laboratories, Kyoto, Japan in 1997. From 2000 to 2002, he worked for NTT DOCOMO, Yokosuka, Japan. In 2002, he moved to DOCOMO communications laboratories Europe GmbH, Germany. From 2004 to 2011, he worked as an associate professor at Kyoto University. Since 2011, he is a full professor at Okayama University. From the beginning of his research career, he has been engaged in the research and development of digital mobile radio communications. In particular, he has considerable interests in channel equalization, array signal processing, Space time codes, spatial multiplexing, and multimode reception. He won the Best paper award of the 19th international symposium on wireless personal multimedia communications (WPMC2016), and the outstanding paper award of the 23rd international conference on advanced communications technology (ICAT2021). He received the excellent paper award and the best paper award from the IEICE in 1995 and from the IEICE communication society in 2020, respectively.

Shuhei Makabe received B.S. and M.S. degrees from Okayama University, Japan, in 2021 and 2023, respectively. He joined with Nippon Telegraph and Telephone West Co. Ltd., in 2023. His research interests include signal processing, wireless communication systems, and overloaded MIMO systems.

Yafei Hou received his Ph.D. degrees from Fudan University, China and Kochi University of Technology (KUT), Japan in 2007. He was a post-doctoral research fellow at Ryukoku University, Japan from August 2007 to September 2010. He was a research scientist at Wave Engineering Laboratories, ATR Institute International, Japan from October 2010 to March 2014. He was an Assistant Professor at the Graduate School of Information Science, Nara Institute of Science and Technology, Japan from April 2014 to March 2017. He became an assistant professor at Okayama University, Japan from April 2017. He is a guest research scientist at Wave Engineering Laboratories, ATR Institute International, Japan from October 2016. His research interest are communication systems, wireless networks, and signal processing. He received IEICE (the Institute of Electronics, Information and Communication Engineers) Communications Society Best Paper Award in 2016, 2020, and Best Tutorial Paper Award in 2017. Dr. Hou is a senior member of IEEE and IEICE.